PHYSICAL REVIEW B **81**, 020412(R) (2010)

Splitting of a moving transverse domain wall in a magnetic nanostripe in a transverse field

S. Glathe, M. Zeisberger, U. Hübner, and R. Mattheis
Institute of Photonic Technology Jena, A.-Einstein-Str. 9, 07745 Jena, Germany

D. V. Berkov
Innovent e.V., Prüssingstr. 27, 07745 Jena, Germany
(Received 19 November 2009; published 26 January 2010)

The field-driven domain-wall dynamics in magnetic nanostripes under the influence of transverse fields was examined experimentally and by numerical simulations. For a small range of transverse fields in a regime below the Walker field an unexpected instantaneous change in the domain-wall velocity was found. Micromagnetic simulations have shown that this peculiar behavior is caused by a transformation of the moving asymmetric transverse wall: the wall is stretched along the nanostripe due to different velocities of the upper and lower half antivortices constituting the domain wall.

DOI: 10.1103/PhysRevB.81.020412 PACS number(s): 75.60.Ch, 75.70.Kw, 75.75.−c

Domain walls (DWs) in nanostripes are the key elements for different spintronic applications. The control of the domain-wall position in magnetic nanostripes by means of magnetic fields[1–7] and electric currents[8–12] was addressed recently in many contributions. These were motivated by possible DW applications for data storage,[13,14] logic devices,[15] and an existing application based on moving DWs in nanostripes, the multiturn counter.[16–18] In most experiments examining the field-driven DW motion a field was applied along the motion direction. DW logic and the multiturn counter are based on DWs, moved through a system of magnetic nanostripes by *rotating* magnetic fields. Understanding of domain-wall dynamics under these conditions is crucial for the application of these devices. Here, besides the longitudinal field component H_{long} (driving the DW through a nanostripe), an additional transverse field H_{tr}, directed in-plane perpendicular to the nanostripe long axis is present during the DW motion. The effect of such a field on the DW dynamics was recently studied in simulations[19,20] and experiments.[6,7] It was shown that a transverse field strongly influences the DW dynamics both below and above the critical Walker field H_w.

In this Rapid Communication we report a dynamic phenomenon appearing at relatively large transverse fields and manifesting itself in an abrupt change in the DW velocity outside the Walker breakdown regime. Micromagnetic simulation has revealed a peculiar DW motion type responsible for the observed behavior.

We have examined the DW motion in $Ni_{81}Fe_{19}$ nanostripes of $w=300$ nm width and $d=10$ nm thickness. These nanostripes were the free layer of giant magnetoresistance (GMR) stacks with the composition Ta(5 nm)/NiFe(10 nm)/CoFe(0.8 nm)/Cu(2 nm)/CoFe(3 nm)/Ru(0.8 nm)/CoFe(3 nm)/IrMn(7 nm)/Ta(5 nm). The stack was deposited on a sapphire substrate using physical vapor dc magnetron sputtering (base pressure $<2\times10^{-8}$ mbar) and patterned by means of e-beam lithography and Ar ion etching. Electrical Al contacts in coplanar waveguide geometry were deposited using a lift-off process.

A sample design is shown in Fig. 1(a). The reference magnetization of the 12-μm-long nanostripe was oriented parallel to its long axis (chosen as x axis). Using the experimental setup sketched in Fig. 1(a), we measured the resistance time dependence in single shot measurements. The GMR value is a direct measure of the sense layer magnetization component m_{long} parallel to the nanostripe long axis so that we could track the DW during its movement. For the present Rapid Communication we have used the following procedure. After saturating the NiFe layer in the stripe direction by using a longitudinal field $H_{\text{long}}=-40$ kA/m, we applied first a constant transverse field H_{tr} and then a linearly increasing longitudinal field $[dH_{\text{long}}/dt\approx160$ (kA/m)/s]. Note that during DW motion ($\ll1$ μs) the longitudinal field is practically constant. Both the critical longitudinal field $H_{\text{long}}^{\text{cr}}$ required to nucleate a DW and the DW velocity v_{DW} (measured in this field $H_{\text{long}}^{\text{cr}}$) exhibited a strong dependence on the transverse field H_{tr} as shown in Fig. 1(b). The continuous decrease in H_{long} with increasing H_{tr} is discussed in detail in Ref. 6.

Figure 2(a) shows single shot measurements at transverse fields marked as A and B in Fig. 1(b). For large H_{long} (case A, $H_{\text{long}}^{\text{cr}}=9.8$ kA/m and $H_{\text{tr}}=6$ kA/m) we can clearly resolve the stop-and-go motion typical for the Walker breakdown process. When the transverse field is increased to $H_{\text{tr}}=8.6$ kA/m, then the longitudinal field necessary for

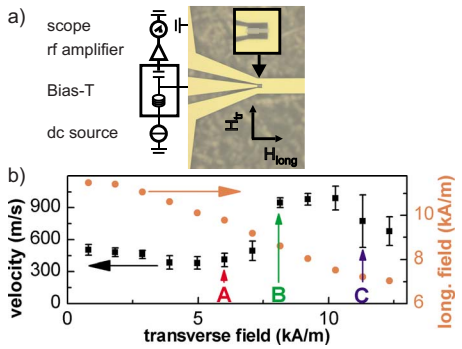

FIG. 1. (Color online) (a) Measurement setup and a micrograph of the GMR device. The inset shows the GMR nanostripe. (b) The DW mean velocity (squares) and longitudinal field (circles) $H_{\text{long}}^{\text{cr}}$ as a function of H_{tr} (averaged over 25 repetitive measurements at each H_{tr}). Error bars for $H_{\text{long}}^{\text{cr}}$ are smaller than the symbol size.

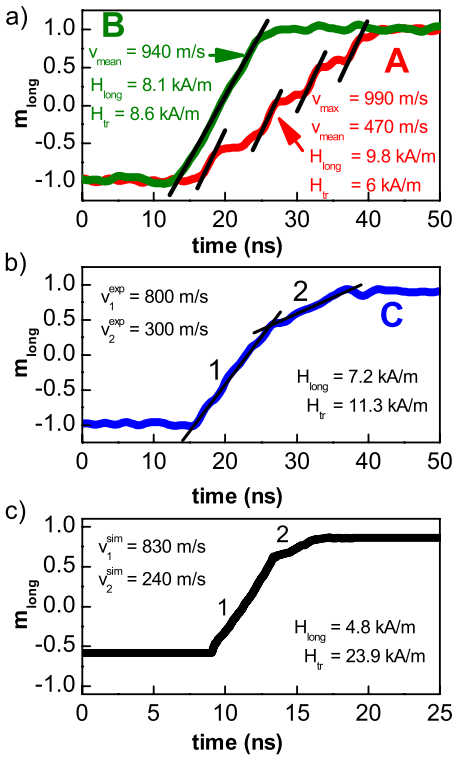

FIG. 2. (Color online) Time dependencies of the longitudinal magnetization $m_{\mathrm{long}}(t)$ for field values as shown in the legend: [(a) and (b)] experiment (nanostripe dimensions $10\times300\times12\,000$ nm^3), (c) simulation ($10\times200\times6000$ nm^3 nanostripe). $m_{\mathrm{long}}(t)$ dependencies were used to calculate the DW velocities given on the figure.

nucleation decreases to $H_{\mathrm{long}}^{\mathrm{cr}}=8.1$ kA/m and the DW moves without oscillations. This indicates a suppression of the Walker breakdown process due to the combined action of transverse and longitudinal fields.[6,7,20] Hence the mean DW velocity increases drastically as shown in Fig. 1(b).

Increasing H_{tr} above 10 kA/m, we observed a decrease in the DW velocity and a strong increase in its dispersion, which achieves a maximum around $H_{\mathrm{tr}}=11.3$ kA/m [marked with C in Fig. 1(b)]. This observation qualitatively differs from the behavior reported previously[6] for the nanostripe with the dimensions $w=160$ nm and $d=20$ nm. Namely, in Ref. 6 after the Walker breakdown was suppressed at a sufficiently large transverse field, we observed the continuous and nonlinear increase in the DW velocity when H_{tr} was increased further.

To understand the reason for the decrease in the DW velocity and increase in its dispersion in the present Rapid Communication, we show a typical single shot measurement of the DW movement for $H_{\mathrm{tr}}=11.3$ kA/m and $H_{\mathrm{long}}=7.2$ kA/m [Fig. 2(b)]. One can see that the m_{long} slope changes abruptly during the DW motion. The velocities calculated from the two slopes (marked with 1 and 2) of the $m_{\mathrm{long}}(t)$ dependence, are $v_1^{\mathrm{exp}}=800$ m/s and $v_2^{\mathrm{exp}}=300$ m/s. Such abrupt changes in the DW velocity during its movement *below* the Walker breakdown cannot be explained, up to our knowledge, with existing theories of DW dynamics. This behavior does not occur for every of the 25 measurements at $H_{\mathrm{tr}}=11.3$ kA/m. In some case the DW moves through the nanostripe with constant (high) velocity. These strong differences in the DW behavior for different measurements at the same H_{tr} causes the large dispersion of the DW velocity.

In order to clarify this peculiar feature of the DW motion, we have performed micromagnetic simulations for the system similar to that used experimentally using the MICROMAGUS package.[21] We have simulated the DW dynamics in a 10×200 (and 300, respectively) $\times6000$ nm^3 nanostripe using discretization cells of $10\times5\times5$ nm^3. The material parameters are chosen as for Permalloy ($M_s=750$ kA/m, $A=1.3\times10^{-11}$ J/m). In the starting configuration of our simulations the DW is pinned to an artificial notch in the nanostripe, positioned 1 μm apart from the left stripe edge; for this reason the magnetization at $t=0$ is $m_{\mathrm{long}}=-0.6$ (and not -1.0).

We note that simulations were performed for the perfect nanostripe shape, i.e., not taking into account the nanostripe edge roughness, present in real systems. An edge roughness decreases the effective nanostripe width and influences the DW dynamics significantly, causing, e.g., a shift of the Walker field.[22] Therefore, the quantitative agreement between the DW dynamics found experimentally and in simulations cannot be expected even for nanostripes having the same dimensions. As mentioned above, we performed the simulations for two different nanostripe widths −200 and 300 nm. In both cases we have found this type of DW behavior (of course, for different field values). However, in the 300-nm-wide nanostripes the DW dynamics demonstrates a much wider variety than for the 200 nm stripes (which will be published elsewhere). Thus, in order to simplify the explanation, we concentrate in the following on the simulations of the 200-nm-wide nanostripes.

In previous micromagnetic studies where small transverse fields were used,[19,20] the type of the DW dynamics found here has not been reported so that the transverse field strength seems to play a key role. Hence we have studied the DW motion in dependence on H_{tr}. Detailed results of this study will be reported elsewhere. Here we present a typical example for a transverse field $H_{\mathrm{tr}}=23.5$ kA/m (and $H_{\mathrm{long}}=4.8$ kA/m). The time dependence $m_{\mathrm{long}}(t)$ for the parameters specified above is shown in Fig. 2(c). This simulated dependence is remarkably similar to that found experimentally [shown in Fig. 2(b)]. The velocity also changes instantaneously, dropping from the large initial value of $v_1^{\mathrm{sim}}=830$ m/s to $v_2^{\mathrm{sim}}=240$ m/s.

Visualization of the simulated magnetization configurations (see Fig. 3) immediately reveals the reason for this highly nontrivial magnetization time dependence and the abrupt change in the effective DW velocity. Namely, it can be clearly recognized, that after the DW starts to move, it quickly splits into two parts, and the upper part moves much faster than the lower one. As long as both parts remain within the nanostripe, the total longitudinal magnetization component changes very fast, resulting in the large apparent DW velocity, calculated as $v_{\mathrm{DW}}\propto dm_{\mathrm{long}}/dt$. When the upper DW part, moving much faster, reaches the right nanostripe end, the magnetization component m_{long} continues to change but due to the motion of the lower DW part only. Hence the

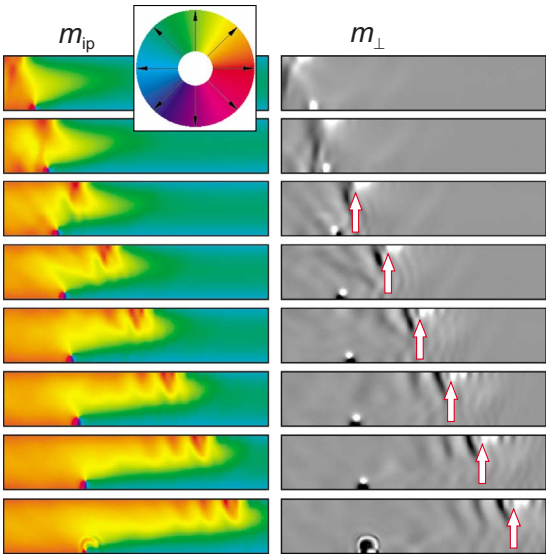

FIG. 3. (Color online) Snapshots of the simulated magnetization configurations of a 6-μm-long nanostripe during the DW movement for H_{tr}=23.9 kA/m and H_{long}=4.8 kA/m. Images show a 1 μm long cutoff of the strip. Time interval between the images is Δt=0.1 ns. Arrows on the grayscale maps of $m_{\perp}$ projections show the exact locations of the leading half antivortex formed at the upper part of the split DW.

change rate dm_{long}/dt becomes much smaller, resulting in the abrupt decrease in the calculated v_{DW} [Figs. 2(b) and 2(c)].

In order to understand this behavior, we note first that for magnetic and geometric parameters used in simulations, the DW formed at t=0 (when only H_{tr} is applied) is the so-called asymmetric transverse wall.[6,23] This wall is formed by two half antivortices (HAVs) with opposite winding numbers n: the upper HAV with n=+1/2, and a lower HAV with n=−1/2.[24] For the asymmetric transverse wall these two HAVs are shifted with respect to each other in the longitudinal direction.

Due to the different magnetization rotation senses within the upper and lower HAVs, they have very different stray field energies. This leads to the different widths of the two HAVs (clearly visible already in the equilibrium state[6,23]). This difference also leads to different mobilities of the two HAVs in the longitudinal applied field so that the upper HAV moves initially faster than the lower one.

The last statement is qualitatively true both in the presence and absence of a transverse field. However, when H_{tr} is absent, the initially fast motion of the upper HAV slows down when the DW continues to move, and then the motion direction of the upper HAV is even reversed (see Fig. 4). This process, combined with the formation of the full antivortex and its periodic motion across the nanostripe, leads to the well-known periodic oscillations of the magnetization components, observed in simulations of the transverse wall dynamics in a nanostripe (see, e.g., Refs. 23 and 25).

In contrast, our simulations show, that in a sufficiently large transverse field the upper DW part *always* moves faster than the lower one. We note also that in presence of H_{tr} the full antivortex (AV) is also formed at the nanostripe edge where the HAV with the lower mobility is located (as for

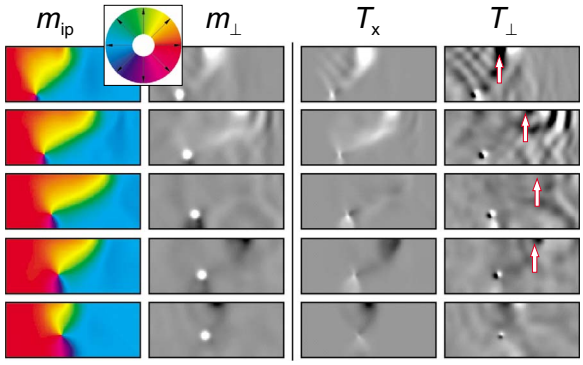

FIG. 4. (Color online) Snapshots of the simulated magnetization configurations (first two columns) and longitudinal and out-of-plane torque components (third and fourth columns) during the DW motion in a nanostripe for H_{long}=4.8 kA/m in the absence of a transverse field. The length of the displayed strip region is 500 nm; images are taken at time intervals Δt=0.2 ns. Arrows on the grayscale maps of $T_{\perp}$ projections show the exact locations of the upper half antivortex.

H_{tr}=0). However, this AV never reaches the opposite nanostripe edge—it is pushed back to its initial position, where it annihilates, emitting a burst of spin wave (see last picture row in Fig. 3).

The analytical theory, which would allow us to understand, why the increase in the transverse field value qualitatively changes the DW dynamics is, up to our knowledge, not available. In particular, we cannot calculate the mobility of the two HAVs mentioned above, especially for the case, when an additionally transverse field is applied. For this reason, we can present only qualitative arguments explaining why the application of H_{tr} is crucially important.

From the "energetic" point of view the explanation for the DW splitting is relatively straightforward. When the upper HAV at the initial stage of the DW motion moves forward faster than the lower HAV, the wall is tilted and stretched along the nanostripe direction as it can be seen at the first three image rows in Fig. 4. The magnetization in the tilted part of the domain wall is directed in plane and nearly perpendicular to the x axis. When the transverse field H_{tr} is applied, its direction coincides with the magnetization direction in this tilted DW part, thus leading to a large gain in the Zeeman energy. When the magnitude H_{tr} reaches a critical value, this energy gain compensates the exchange energy increase due the wall elongation. Hence the formation and growth of the wall region parallel to the long strip side becomes energetically favorable, resulting in the DW splitting as shown in Fig. 3.

However, for the small damping typical for real NiFe layers studied in our experiments (in simulations we have used α=0.01) the DW motion is essentially a dynamic process governed by the magnetization precession, so that the "energetic" argument presented above is not enough to explain the qualitative change in the DW dynamics when H_{tr} is switched on.

To better understand the transverse field influence on the DW dynamics, we have to recapitulate in more details the behavior of the upper (initially faster) HAV during the DW

motion without a transverse field. The important point is that when this half antivortex moves (initially) to the right, its velocity decreases, then the HAV stops and starts to move in the opposite direction. This process can be clearly seen on the color maps of the in-plane magnetization projection (first column in Fig. 4). The reason for this change in the movement direction is the gradual change in the HAV polarity during its motion. Namely, initially the HAV-core magnetization points along the positive out-of-plane direction (bright spots showing the HAV position at the first two $m_\perp$ maps in Fig. 4), then the out-of-plane component of the HAV magnetization reduces and finally changes its sign as it can be seen from the dark spots marking the HAV on the last two $m_\perp$ maps in Fig. 4. The detailed analysis (which will be reported elsewhere) shows that T_x component of the torque responsible for the longitudinal HAV motion is dominated by demagnetizing field torque $\mathbf{T}_{\mathrm{dem}}$. Hence, when the $m_\perp$ component of the HAV core changes sign, T_x component changes its sign also, thus causing the backward HAV motion (see the third column in Fig. 4).

The decrease and the sign change in the initially positive $m_\perp$ component is caused, in turn, by the out-of-plane torque projection $T_\perp$: dark spots indicated by arrows on the first two $T_\perp$ maps in Fig. 4 clearly show that this component is negative at the HAV location. The detailed analysis shows that the (negative) out-of-plane torque projection is a result of the nearly cancellation of the demagnetizing $\mathbf{T}_{\mathrm{dem}}$ and exchange torques $\mathbf{T}_{\mathrm{exch}}$, whereby the magnitude of $\mathbf{T}_{\mathrm{exch}}$ is slightly larger.

When, in addition, a transverse field is applied, it makes a magnetization configuration more homogeneous. The first important point is that this has a larger impact on the exchange torque $\mathbf{T}_{\mathrm{exch}}$ (compared to $\mathbf{T}_{\mathrm{dem}}$) because $\mathbf{T}_{\mathrm{exch}}$ is proportional to the spatial *derivatives* of the magnetization components. Second, for the same reason, the magnitude $\mathbf{T}_{\mathrm{exch}}$ reduces with increasing H_{tr} [because $\mathbf{M}(\mathbf{r})$ becomes more homogeneous]. Hence, starting from some value of H_{tr}, the exchange torque component $T_\perp^{\mathrm{exch}}$ at the HAV location is not more able to overcompensate the positive demagnetizing torque $T_\perp^{\mathrm{dem}}$. Thus the $m_\perp$ component of the HAV core remains positive as it can be seen on the $m_\perp$ maps in Fig. 3, where the HAV positions are marked by the arrows. For this reason the upper HAV velocity is always positive and exceeds the velocity of the lower HAV causing the DW splitting.

In conclusion, we have found a peculiar type of the DW dynamics in a nanostripe under the influence of an in-plane transverse field. Due to this field the upper and lower half antivortices of the transverse wall can behave as independent quasiparticles. The different mobilities of these two half-antivortices results in different velocities of the two corresponding DW parts in the given longitudinal field. This leads to an abrupt change in the *effective* DW velocity measured from the time dependence of the total longitudinal magnetization component.

We acknowledge the financial support by German Ministry of Education and Research under Grant No. 13 N 10125 and by company Novotechnik Ostfildern/Germany.

[1] T. Ono, H. Miyajima, K. Shigeto, K. Mibu, N. Hosoito, and T. Shinjo, Science **284**, 468 (1999).
[2] K. Kondou, N. Ohshima, S. Kasai, Y. Nakatani, and T. Ono, Appl. Phys. Express **1**, 061302 (2008).
[3] G. S. D. Beach, C. Nistor, C. Knutson, M. Tsoi, and J. L. Erskine, Nature Mater. **4**, 741 (2005).
[4] P. Möhrke, T. A. Moore, M. Kläui, J. Boneberg, D. Backes, S. Krzyk, L. J. Heyderman, P. Leiderer, and U. Rüdiger, J. Phys. D **41**, 164009 (2008).
[5] D. Atkinson, D. A. Allwood, G. Xiong, M. D. Cooke, C. C. Faulkner, and R. P. Cowburn, Nature Mater. **2**, 85 (2003).
[6] S. Glathe, I. Berkov, T. Mikolajick, and R. Mattheis, Appl. Phys. Lett. **93**, 162505 (2008).
[7] S. Glathe, R. Mattheis, and D. V. Berkov, Appl. Phys. Lett. **93**, 072508 (2008).
[8] M. Kläui, C. A. F. Vaz, J. A. C. Bland, W. Wernsdorfer, G. Faini, E. Cambril, L. J. Heyderman, F. Nolting, and U. Rüdiger, Phys. Rev. Lett. **94**, 106601 (2005).
[9] M. Tsoi, R. E. Fontana, and S. S. P. Parkin, Appl. Phys. Lett. **83**, 2617 (2003).
[10] J. Grollier, L. Lacour, V. Gros, A. Hamzic, A. Vaures, A. Fert, D. Adam, and G. Faini, J. Appl. Phys. **92**, 4825 (2002).
[11] A. Yamaguchi, T. Ono, S. Nasu, K. Miyake, K. Mibu, and T. Shinjo, Phys. Rev. Lett. **92**, 077205 (2004).
[12] M. Yamanouchi, D. Chiba, F. Matsukura, and H. Ohno, Nature (London) **428**, 539 (2004).
[13] S. S. P. Parkin, M. Hayashi, and L. Thomas, Science **320**, 190 (2008).
[14] R. Cowburn and D. Allwood, *Multiple layer magnetic logic memory device* (2005).
[15] D. A. Allwood, G. Xiong, C. C. Faulkner, D. Atkinson, D. Petit, and R. P. Cowburn, Science **309**, 1688 (2005).
[16] M. Diegel, R. Mattheis, and E. Halder, Sens. Lett. **5**, 118 (2007).
[17] M. Diegel, R. Mattheis, and E. Halder, IEEE Trans. Magn. **40**, 2655 (2004).
[18] M. Diegel, S. Glathe, R. Mattheis, M. Scherzinger, and E. Halder, IEEE Trans. Magn. **45**, 3792 (2009).
[19] A. Kunz and S. C. Reiff, J. Appl. Phys. **103**, 07D903 (2008).
[20] M. T. Bryan, T. Schreffl, D. Atkinson, and D. A. Allwood, J. Appl. Phys. **103**, 073906 (2008).
[21] D. V. Berkov and N. L. Gorn, *Micromagus: Package for Micromagnetic Simulations*, http://www.micromagus.de
[22] Y. Nakatani, A. Thiaville, and J. Miltat, Nature Mater. **2**, 521 (2003).
[23] A. Thiaville and Y. Nakatani, *Spin Dynamics in Confined Magnetic Structures III* (Springer, New York, 2006), Chap. Domain-Wall Dynamics in Nanowires and Nanostrips, p. 161.
[24] O. Tchernyshyov and G.-W. Chern, Phys. Rev. Lett. **95**, 197204 (2005).
[25] J.-Y. Lee, K.-S. Lee, S. Choi, K. Y. Guslienko, and S.-K. Kim, Phys. Rev. B **76**, 184408 (2007).